University of Thi -Qar Journal for Engineering Sciences
http://www.doi.org/10.31663/tqujes.12.2.445(2022)
Vol 12.2(December 2022)

ISSN :2664- 5572 (online)
ISSN:2664-5564 (print)
Available at http://jeng.utq.edu.iq
utjeng@ utq.edu.iq

A SiC-based Rectifier for SCR-based Rectifiers Replacement to Improve the Performance of the Static Exciters in the QAWTP

Hassan Athab[†], Abdul-Hamid Al-Hilfi[‡] and Kadum Abneyan[ł]
[†]Rumaila Operation Organization, hassanathab@gmail.com.
[‡]Al-Baidak Al-Aswad Company, alhlfi705@yahoo.com.
[ł]Basra Oil Company, kadumabneyan@gmail.com.

Abstract

Due to the thyristors drawbacks, the obsolete driving and control hardware spare parts, and instead of replacing the entire excitation systems, this paper proposes a SiC-based rectifier as a replacement for the SCR-based rectifiers that are used in the exciters to provide the DC field current to the rotors of the synchronous motors in Qarmat-Ali Water Treatment Plant (QAWTP). The system performance is improved and its power density is enhanced by improving the rectifier performance. In addition to the capability to operate in harsh environments and high ambient temperatures, the proposed rectifier minimizes the harmonic contents in the input current and the output voltage. The rectifier is simulated with a maximum current of 200 A which is higher than the current that is measured in the station. The calculated efficiency of the rectifier is about 90%. With a small input passive filter, the archived THD of the input current is 11% with a light load and 22% with a full load.
Keywords: Exciter, half-controlled rectifier, thyristor, Silicon-Carbide.

1. Introduction

Water injection is essential in the oil industry for ensuring production by maintaining the reservoir's pressure at certain levels and increasing production by boosting the reservoir's pressure levels. In Rumaila, the annual water injection rate had been increased from 200 thousand barrels per day in 2013 to more than 1400 thousand barrels per day in 2021 **[1]**. The water is filtered and passed through different treatment operations in the Qaramt Ali stations, before exporting it to the Cluster Pump Stations (CPSs) to be injected into the reservoir. The water is exported to the Rumaila oil fields by centrifugal pumps. There are nine pumps each pump is driven by a 2.5 MW synchronous motor which is shown in Fig. 1, the motor specifications are given in Table 1. Although synchronous machines have many advantages like the constant angular speed regardless
the load and the power factor controllability, they are not preferred in most of the applications due to their high cost compared with their counterpart of induction motors, lack of self-starting, and the requirement of two types of sources, an AC source that feeds the stator and a DC source that feeds the rotor.
The devices that provide the DC current to the rotors are known as exciters; Fig. 2 shows the excitation system panel that is used in the station. Besides their main function which is applying the excitation field and the protection functions such as over and under excitation, motor pullout protection and incomplete sequence, excitation systems provide a discharge path for the induced current in the rotor. Meanwhile, the field current is controlled depending on the operation modes includeeactive power control mode, voltage droop control mode and Volt/Herts limiting mode.

Fig.1 2.5 MW 6.6 kV synchronous motor

All the rectifiers that are used in the existing exciters are based on thyristors. Generally, these thyristor-based rectifiers have many disadvantages such as low power factor due to the high reactive consumption and high input current distortion. More importantly, some of the spare parts for the thyristors' deriving boards and the control circuits are either obsolete or very expensive.

Table 1 Motor parameters **[2]**.

No.	Parameter	Rated Value
1	Effective output power	2500 kW
2	Stator Voltage	6600 V
3	Stator Current	252 A
4	Frequency	50 Hz
5	Rotation Frequency	1000 rpm
6	Rotor Voltage	58 V
7	Rotor Current	220 A
8	Winding Resistance at	Stator: 79.1 mΩ

	20°C	Rotor: 188 mΩ
9	Air Gap Mean Value	9 mm

On the other side, the fluctuating in the motor output power due to the change in quantity and the pressure of water in the pipes or due to the changing of the supply voltage requires a fast response rectifier to adjust the field current to compensate for the power variations. The relationship between the field voltage and the power is explained in detail in the next section. The response of the thyristors-based rectifiers is very slow that makes them not suitable for such applications, especially where the utility voltage and frequency are not stable. Therefore, the approach is to design a replacement for these rectifiers rather than replacing the entire excitation system. The proposed rectifier is based on Silicon Carbide MOSFETs which improve the exciters' performance and provide more flexibility and controllability to the systems.

Fig.2 Excitation system panel

2. Excitation and Output Power Relationship

Since the poles of the rotor are salient, the motor's reactance varies depending on the rotor position because of the non-uniform air-gap **[3]**. Reluctance torque develops because of the pole saliency. Therefore, the magnetic of the stator is represented by two axes, a direct axis which is aligned with the rotor axis and a quadrature axis which is perpendicular to the rotor axis. Based on the equivalent circuit which is illustrated in Fig. 3(a), the terminal phase voltage (Vt) is given by:

$$\bar{V}_t = \bar{E}_f + \bar{I}_a R_a + jI_d(X_d + X_{le}) + jI_q(X_q + X_{le}) \quad (1)$$

Where E_f is the phase value of the induced electric motive force (EMF) which depends on the field current that is provided by the exciter, I_a is the armature current, Ra is the armature resistance, X_d and X_q are the direct and quadrature reactance component respectively, and X_{le} is the stator leakage reactance. The current components for the leading power factor are obtained as:

$$I_d = I_a \sin(\delta + \varphi) \quad (2)$$
$$I_q = I_a \cos(\delta + \varphi) \quad (3)$$

Where δ is the angle between the EMF and Vt and ϕ is the power factor angle. These parameters are illustrated in the phasor diagram in Fig. 3(b). By neglecting the voltage drop across the armature resistance and the leakage reactance, the induced voltage can be approximated as:

$$E_f \approx V_t \cos(\delta) + I_d X_d \quad (4)$$

Thus, the active and reactive powers are obtained by:

$$P = \frac{3V_t E_f}{X_d} \sin(\delta) + \frac{3V_t^2}{2}\left(\frac{1}{X_q} - \frac{1}{X_d}\right) \sin(2\delta) \quad (5)$$

$$Q = \frac{3V_t E_f}{X_d} \cos(\delta) - 3V_t^2\left(\frac{\cos^2(\delta)}{X_d} + \frac{\sin^2(\delta)}{X_q}\right) \quad (6)$$

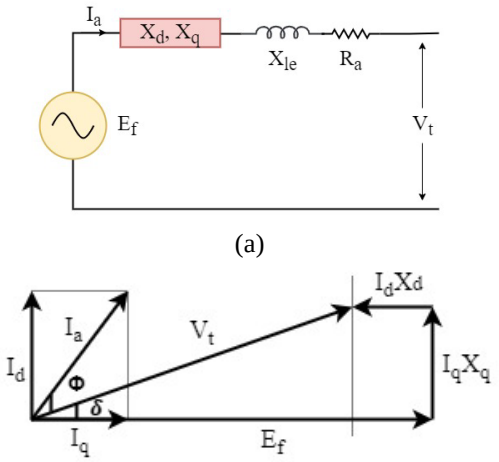

Fig.3 (a) Salient Pole synchronous motor equivalent circuit (b) leading power factor phasor diagram

3. System Description

These motors are operated by a direct on-line method when the stator windings are connected to the grid by closing the circuit breaker. Each exciter is fed by a 3-ph 50 kVA step-down transformer whose primary windings are connected in parallel with the stator as shown in Fig. 4. The AC voltage of the secondary windings of the transformer is rectified by an SCR-based three-phase rectifier. The output of the rectifier is connected to the field windings through carbon brushes and slip-rings. The DC voltage is controlled by adjusting the thyristors firing angles. The average output voltage is given by **[4]**:

$$V_{dc} = \frac{3}{\pi}\int_{\frac{\pi}{6}+\alpha}^{\frac{\pi}{2}+\alpha} v_{ab}\, d(wt)$$
$$= \frac{3}{\pi}\int_{\frac{\pi}{6}+\alpha}^{\frac{\pi}{2}+\alpha} \sqrt{3}V_m \sin\left(wt + \frac{\pi}{6}\right) d(wt)$$
$$= \frac{3\sqrt{3}V_m}{\pi}\cos\alpha \quad (7)$$

Where α is the firing angle, v_{ab} is the line-to-line voltage and V_m is the voltage magnitude. Notably, the maximum average output voltage is obtained when α = 0.

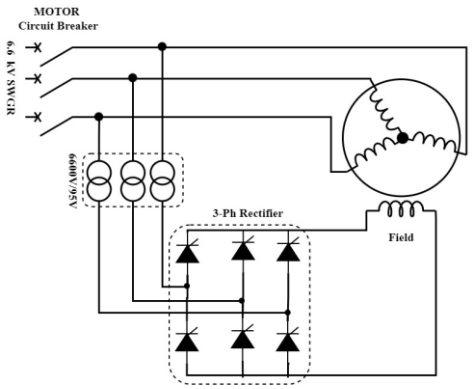

Fig.4 Synchronous motor with SCR-based excitation system

Although thyristors have lower on-state conduction losses and higher power handling capability, in addition to the aforementioned disadvantages they suffer from other drawbacks such as the lack of turning-off capability and slow switching. Consequently, the line commutated rectifiers, which are built by using SCRs, consume high reactive power and generate more harmonics. The performance of these rectifiers is influenced by the AC side line inductance. The overlap duration among the thyristors is directly proportional to the line inductance. Depending on the motor parameters and the transformer turn ratio of the existing system, it is found that the minimum firing angle is about 63° in order to meet the rotor-rated voltage. Operating with large firing angles leads to higher harmonic distortions. Fig. 5 shows the FFT analysis (the fundamental component is not included) of the rectifier output voltage and the input current when the firing angle is the allowable minimum value. Thus, the thyristor-based
exciters pollute the power system with harmonics of the input current as well as the output voltage. The harmonics in the field voltage have a negative impact on the rotor winding in addition to degrading the motor performance.

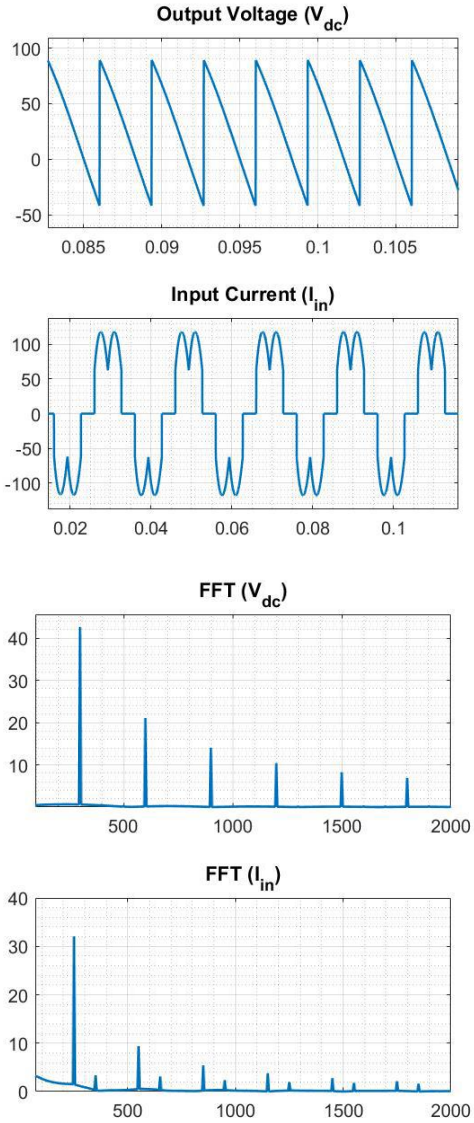

Fig.5 Output voltage and input current of the Thyristor-based rectifier with 200 A output field current

4. Silicon Carbide-based Rectifiers

Silicon Carbide power devices have many advantages such as fast switching frequency, low power losses, small leakage current, and high operating junction temperature **[5]**. Therefore, they are used in different applications such as high voltage direct current transmission **[6]**, solar systems **[7]**, wind energy systems **[8]**, and electric and hybrid electric vehicles **[9]** and **[10]**. In **[11]**, a 5 kW 380 VAC input 800 VDC output All-SiC three-phase active front-end boost PWM rectifier is compared with All-Si and hybrid rectifiers. It is found that the All-SiC is 1.2% more efficient than the All-Si and 0.5% more efficient than the hybrid device. A comparison between SiC-based current source rectifier (CSR) and voltage source rectifier (VSR) for DC microgrid applications is presented in **[12]**. The rated power of each rectifier is 30 kW and they operate with a 40 kHz switching frequency. The analysis shows that CSR efficiency and power density are higher than VSR. SiC MOSFETs with Schottky diodes are used

to build a 7.5 kW three-phase buck rectifier with 480 Vrms input and 400 Vdc output voltage for the data center power supply is presented in **[13]**. The rectifier achieves 98.5% efficiency at full load. Unlike the previous rectifiers that use normally-off transistors, normally-on SiC JFETs are implemented in **[14]** to construct a rectifier prototype, the rectifier achieves a 91.4% nominal efficiency.
Accordingly, the characteristics of the SiC-based power transistors make them more suitable for harsh environments like the Rumaila oil field environment. Based on the motor parameters that are given in Table 1 and taking into consideration the availability and the cost of the switching devices and the other components, the SiC-based half-controlled rectifier (semi-converter) which is shown in Fig. 6, is chosen as a replacement topology for the existing thyristor-based full-controlled rectifier.

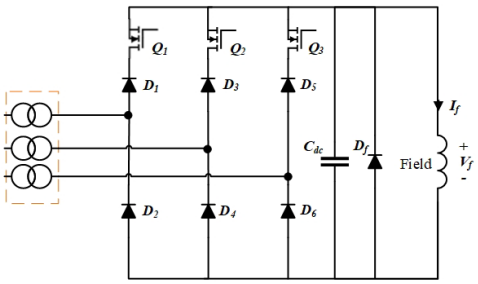

Fig.6 Half-controlled rectifier

5. Semi-Converter-based Exciter

In addition to the power loss reduction, a semi-converter that is demonstrated in Fig. 6 can increase the system power density due to the smaller number of controlled switches (only three transistors) and auxiliary circuits like driving circuits, and snubber circuits that are utilized. The MOSFET-based half-controlled rectifier can operate in two modes. In the first mode, the transistors are switched with a frequency equal to the line frequency (50 Hz) and the dc voltage is controlled by adjusting the on-time (t_{on}) of the MOSFETs. Although this mode reduces the switching losses, it is not considered because it generates low-order harmonics. In the second mode, the switching frequency is high so the low-frequency harmonics are reduced and the generated harmonics can be eliminated by using a small LC low-pass filter. Since SiC-based MOSFETs and diodes are exploited, the passive components of the filters can be further minimized due to the high switching frequency. Unfortunately, the half-controlled rectifier inherently produces even harmonics **[15, 16]** due to the irregularities in the on-times between the upper switches (diodes and transistors) and lower switches (diodes). The magnitude of the generated even harmonics by the proposed is not large; therefore, their impact on the performance of the system is negligible.
The used switching sequence is similar to the sequence of the conventional rectifiers. Based on the input voltage that is shown in Fig. 7, diodes (D_1 and D_6) and the MOSFET (Q_1) are ON during the period ($\pi/6 - \pi/2$), D_6 turns OFF when the voltage of phase 3 increases after Π/2 and the current will flow through D_4. At 5π/6, Q_1 and D_1 turn OFF and Q_2 and D3 will be ON. D_4 turns OFF and D2 will be ON during the period ($7\pi/6 - 11\pi/6$). Finally, the period between (3π/2 and 13π/6), Q_3 and D_5 are ON and the rest of the upper switches are OFF.

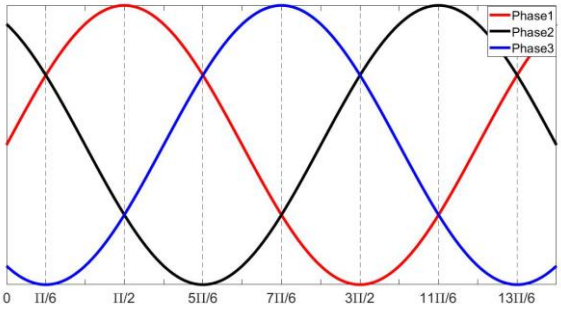

Fig.7 Three-phase input voltage

The system power losses can be divided into two categories: the semiconductor losses, the power losses in the MOSFETs and diodes; and the passive losses, the losses in the inductors, capacitors, and damping resistors. Only the power that is dissipated in the bridge is considered. In other words, the power losses in the switches (Q1, Q2, and Q3) and the diodes (D1 to D6), which are given by **[17]:**

$$P_{Diode} = V_f * I_{Diode\_av} + R_{Diode}\, I^2_{Diode\_rms} \quad (8)$$

$$P_{mos} = \frac{1}{2} V_{DS} I_{Drain} (t_{on} + t_{off}) f_s + I^2_{Drain\_rms} R_{DS-on} = (E_{on} + E_{off}) f_s + I^2_{Drain\_rms} R_{DS-on} \quad (9)$$

Where P_{Diode} is the power loss in a diode and P_{mos} is the dissipated power in a MOSFET, V_f is the diode forward voltage, I_{Diode_av} and I_{Diode_rms} are diode average and RMS currents, V_{DS} and I_{Drain} are the MOSFET voltage and current at the time of the switching, I_{Drian_rms} is the RMS value of the MOSFET current, and R_{DS-on} is the Drain-Source on-state resistance. E_{on} and E_{off} represent the MOSFET turn-on and turn-off energies which are obtained from the datasheet.
The selected MOSFET is (P3M07013K4 N-channel Enhancement Mode **[18]**) and the diode is (GP3D050A065B **[19]**). From the data sheets, the continuous drain current (Id) of the MOSFET is 100 A when the case temperature is 100°C; therefore, three MOSFETs in parallel are used. On the other hand, four parallel diodes are used, the continuous forward current for each diode is 70 A at 125°C case temperature. Depending on the operation condition of the motors in the station, the maximum field current is 180 A. Therefore, the maximum power losses are considered for 200 A output current. For the losses calculations, the average and RMS values of the voltages and currents are obtained simulatively. The calculated power losses in the diodes equal 617 W, while the MOSFETs switching and conduction losses equal 658 W. Thus, the rectifier efficiency is about 90% which is found from the output power and the total power losses.

6. Simulation Results

To validate the performance of the proposed system, simulations are performed using PSIM. The proposed semi-converter power circuit is shown in Fig. 8. The rectifier rated power is 18 kW and the switching frequency is 50 kHz. The per-phase value of the filter inductor (L_f)and the capacitor (C_f) of the input filter are 500 μH and 10 μF respectively. A 1 Ω resistor is connected in series with the filter capacitor to dampen the oscillation in order to ensure system stability. The upper switches S1, S3, and S5 are constructed from the MOSFETs and diodes and the lower switches S2, S4, and S6 are constructed from diodes. The free-wheeling diode (D_f) is connected in parallel with the 100 μF dc side capacitor (C_d) in order to prevent the capacitor from reverse polarity charging so the rotor current flows through the diode when the capacitor is fully discharged. A pulse width modulation, a sine-wave is

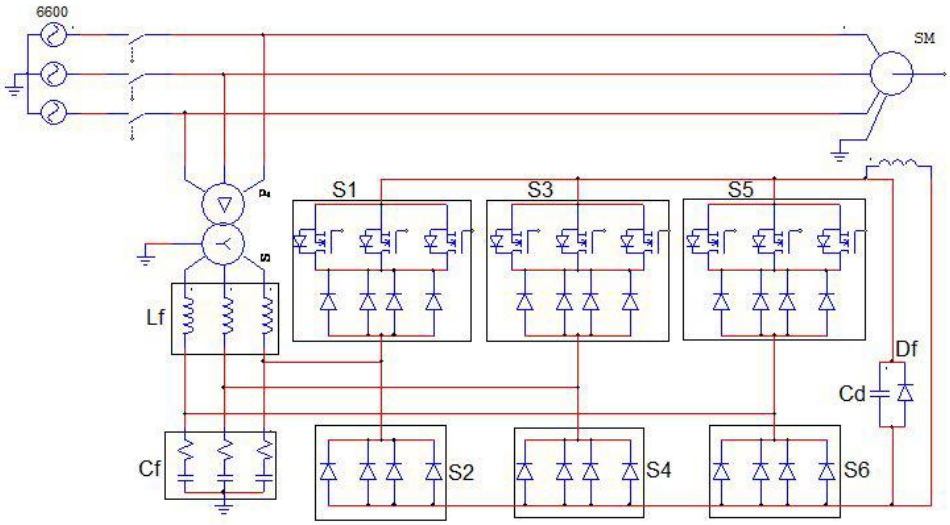

Fig.8 PSIM Half-controlled rectifier power circuit

compared with a triangle carrier signal, is employed to drive the MOSFETs. The phase angle of the fundamental sine-wave is obtained by a phase-locked loop (PLL). The field current is controlled by adjusted rectifier output voltage which is a function of the modulation index.

Fig. 9 shows the output voltage and input current, the current of the secondary winding of the transformer before the LC filter when the field current is about 100 A. From the FFT analysis for the output voltage - the fundamental magnitude is not included - it is seen that the highest magnitudes are the 3rd and 15th but they are small compared to the harmonic magnitudes in the Thyristor-based rectifier output. Although the even harmonics 2nd and 4th occur in the input current as shown lower-right graph in Fig. 9 due to the switches on-time irregularities and the odd harmonic 5th, the total harmonics distortion is 11% which is lower than the distortion that is caused by the SCR-based rectifier.

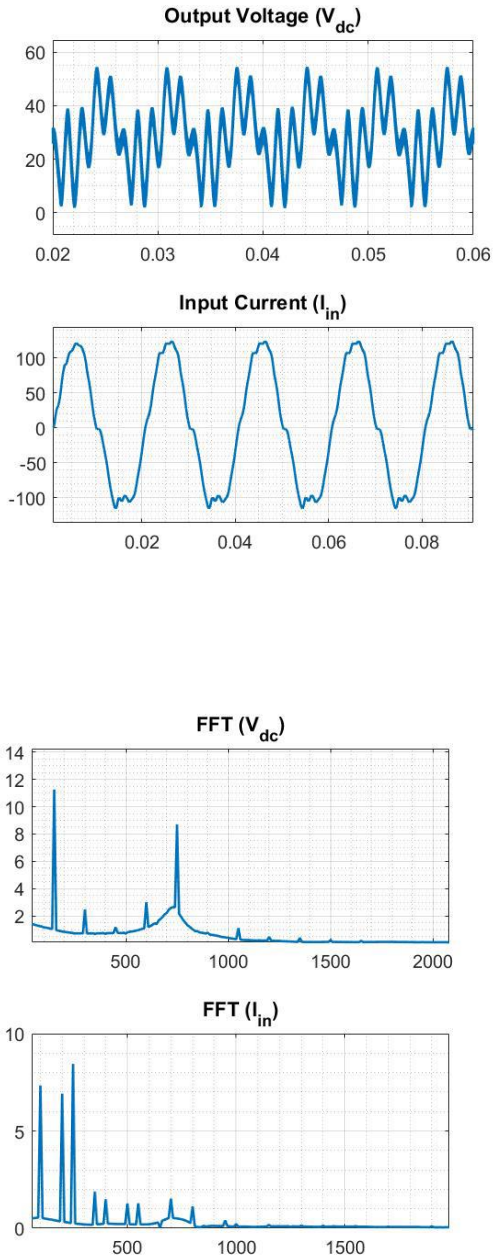

Fig.9 Output voltage and input current of the MOSFET-based rectifier with 100 A output field current

When the average field current is increased to 200 A as shown in Fig. 10, the peak-to-peak current is about 25 A, by adjusting the modulation index, the amplitude of the 15th harmonic becomes very small while the 3rd increases in field voltage as depicted in Fig 11. The 5th harmonic is reduced in the input current but the magnitude of the 2nd harmonic increases therefore the 22% THD is mainly because of the second harmonic.

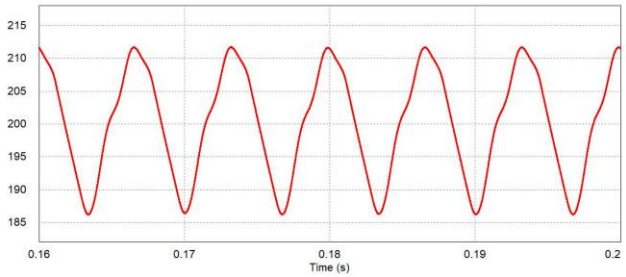

Fig.10 Field current ripple

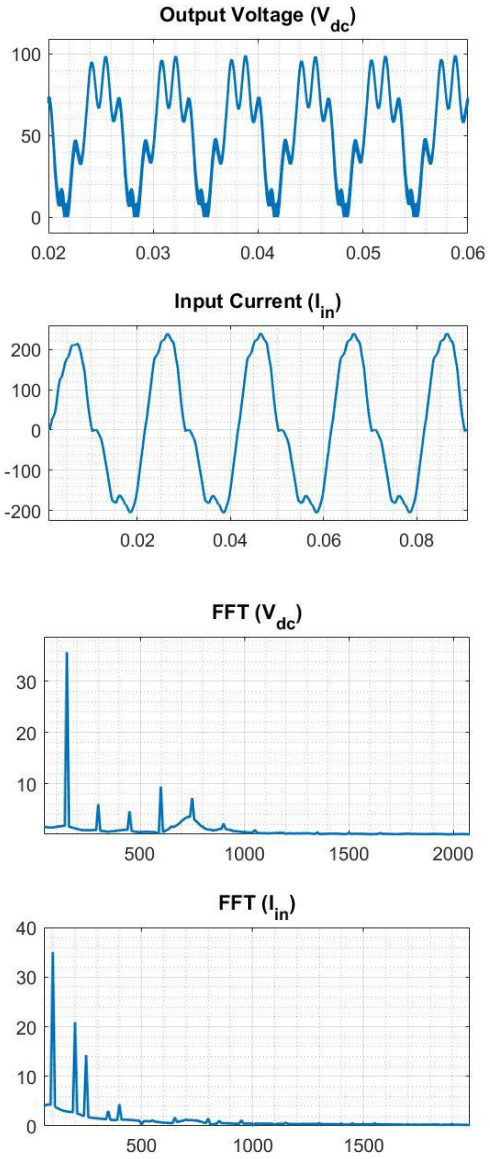

Fig.11 Output voltage and input current of the MOSFET-based rectifier with 200 A output field current

7. Limitation and Future Work

- Some of the motor parameters such as the stator inductance and rotor inductance are not given in the

data sheet and not available online, so they are adjusted to make the operation conditions like what have been observed in the station. This can be solved by obtaining these parameters experimentally.

- Thermal management and heat-sink design have not been considered when the number of parallel switches has been selected. In the future, either the number of parallel switches will be increased or MOSFETs with higher-rated parameters will be selected depending on the thermal requirements.
- The circuit is simulated with open loop control, in the future, a closed loop will be included in order to test the rectifier with rapid change in the input voltage and/or in the motor output power.

Conclusions

The SiC-based half-controlled rectifier can improve the excitation systems' performance in terms of power density, harmonic distortion, and efficiency. The proposed system has a faster response than the SCR-based rectifier; therefore, it is more suitable for weak grids to compensate for voltage and motor power variations besides its ability to operate with higher temperatures. The simulation results verify that the utilized small passive filter is able to mitigate the generated harmonics by the semi-converter. The achieved total harmonics distortion of the input current is 11% with a light load and 22% with a full load. Future works will focus on thermal management and controller design to test the rectifier under different operation conditions.

References

[1] Rumaila Operation Organization, “https://rumaila.iq´´´.
[2] Russiangost,“Available:https://www.russiangost.com/p-18802-gost-183-74.aspx,” [Accessed 6 August 2022].
[3] M. E. El-Hawary, Principles of Electric Machines with Power Electronic Applications,. 397,2002.
[4] M. H. Rashid, Power electronics: devices, circuits, and applications. Pearson, 4th, intern. ed., 2014.
[5] J. Rabkowski, D. Peftitsis, and H.-P. Nee, “Silicon carbide power transistors: A new era in power electronics is initiated,” IEEE Industrial Electronics Magazine, 6. 2,. 17, 2012.
[6] K. Jacobs, S. Heinig, D. Johannesson, S. Norrga, and H.-P. Nee, “Comparative evaluation of voltage source converters with silicon carbide semiconductor devices for high-voltage direct current transmission,” IEEE Transactions on Power Electronics,. 36, 8,. 8887, 2021.
[7] X. She, P. Losee, H. Hu, W. Earls, and R. Datta, “Performance evaluation of 1.5 kv solar inverter with 2.5 kv silicon carbide mosfet,” IEEE Transactions on Industry Applications,. 55,. 6,. 7726, 2019.
[8] M. Abbasi and J. Lam, “A modular sic-based step-up converter with soft-switching-assisted networks and internally coupled high-voltage-gain modules for wind energy system with a medium-voltage dc grid,” IEEE Journal of Emerging and Selected Topics in Power Electronics,. 7, 2,. 798, 2019.
[9] S. Jahdi, O. Alatise, C. Fisher, L. Ran, and P. Mawby, “An evaluation of silicon carbide unipolar technologies for electric vehicle drive-trains,” IEEE Journal of Emerging and Selected Topics in Power Electronics,. 2, 3, 517, 2014.
[10] D. Han, J. Noppakunkajorn, and B. Sarlioglu, “Comprehensive efficiency, weight, and volume comparison of sic- and si-based bidirectional dc-dc converters for hybrid electric vehicles,” IEEE Transactions on Vehicular Technology.. 63, 7, 3001, 2014.
[11] S. Mao, T. Wu, X. Lu, J. Popovic, and J. A. Ferreira, “Three-phase active front-end rectifier efficiency improvement with silicon carbide power semiconductor devices,” in 2016 IEEE Energy Conversion Congress and Exposition (ECCE),. 1, 2016.
[12] Q. Jiao, R. Hosseini, and R. M. Cuzner, “A comparison between silicon carbide based current source rectifier and voltage source rectifier for applications in community dc microgrid,” in 2016 IEEE International Conference on Renewable Energy Research and Applications (ICRERA), 544, 2016.
[13] F. Xu, B. Guo, L. M. Tolbert, F. Wang, and B. J. Blalock, “An all-sic three-phase buck rectifier for high-efficiency data center power supplies,” IEEE Transactions on Industry Applications,. 49,. 6,2662, 2013.
[14] C. J. Cass, R. Burgos, F. Wang, and D. Boroyevich, “Three-phase ac buck rectifier using normallyon sic jfets at 150 khz switching frequency,” in 2007 IEEE Power Electronics Specialists Conference,. 2162, 2007.
[15] P. Buddingh, “Even harmonic resonance - an unusual problem,” in Record of Conference Papers. Industry Applications Society. Forty-Ninth Annual Conference. 2002 Petroleum and Chemical Industry Technical Conference,. 93, 2002.
[16] A. Mansoor, J. McGee, and F. Peng, “Even-harmonics concerns at an industrial facility using a large number of half-controlled rectifiers,” in APEC ’98 Thirteenth Annual Applied Power Electronics Conference and Exposition, 2, 994,.2, 1998.
[17] Ned Mohan, Tore M Undeland, William P Robbins, Power electronics: converters, applications, and design. 2003.
[18] PNJsemi,“Available:http://datasheet.pnjsemi.com/datasheet/mos/p3m07013k4.pdf.,” [Accessed 7 August 2022].
[19] SemiQ,“Available:https://semiq.com/pdf/gp3d050a065b.pdf.,” [Accessed 7 August 2022].